Molecular Recognition of Chiral Diporphyrin Receptor with a Macrocyclic Cavity for Intercalation of Aromatic Compounds[#]

Tadashi Ema,* Norichika Ura, Katsuya Eguchi, and Takashi Sakai*

Division of Chemistry and Biochemistry, Graduate School of Natural Science and Technology, Okayama University, Tsushima, Okayama 700-8530

Received August 2, 2011; E-mail: ema@cc.okayama-u.ac.jp

Chiral diporphyrin receptor **1**, which has a macrocyclic cavity for the intercalation of aromatic guest molecules, was designed and synthesized from pyrrole in five steps. The binding constants (K_a) revealed the greater affinity of **1** for more electron-deficient aromatic guests. The complexation between **1** and 1,3,5-trinitrobenzene (**G8**) ($K_a = 1850\,M^{-1}$) was much stronger than that between porphyrin monomer **3** and **G8** ($K_a = 50\,M^{-1}$). This result strongly suggests that **G8** was intercalated into the cavity of **1** via cooperative double π–π stacking. Interestingly, **1** enabled the naked-eye detection of an aromatic explosive **G8**; a dark-red solution of **1** in $CHCl_3$ turned into a colloidal suspension upon addition of **G8**, and the light was scattered. Fluorescence spectroscopy was also useful for the selective detection of **G8**; fluorescence of **1** was quenched by complexation with **G8**, which was visible with the naked eye. Despite modest binding constants for dinitrobenzene derivatives, **1** showed a good ability to discriminate the enantiomers of twelve chiral compounds bearing a dinitrophenyl group by NMR spectroscopy. The MM calculations with the MM3 force field reproduced inclusion complexes between **1** and nitroaromatic compounds. The mechanism of chiral discrimination is proposed.

Chirality is significant because chiral biomolecules such as proteins, nucleic acids, and carbohydrates play a central role in life. Chiral recognition is also important, and it has been extensively studied.[1] One application of chiral recognition/discrimination is to determine the enantiomeric purity of chiral compounds. NMR chiral shift reagents and chiral solvating agents have been developed for this purpose,[2–4] and we have reported chiral macrocyclic hosts, which use hydrogen bonding as the driving force of complexation.[4] These hosts making use of hydrogen bonds, however, cannot exert chiral discrimination toward guests bearing no hydrogen-bonding sites.

The π–π stacking interaction plays an important role in biomolecules, organic materials, and host–guest complexes.[5–7] The π–π stacking is so weak that other interactions, such as hydrogen bonds, need to be used to increase the host–guest binding affinity.[8] Recently, the π–π stacking interaction has been successfully used in the chiral recognition of fullerenes and carbon nanotubes.[9,10] Because there are few examples that employ π–π stacking as a sole driving force of enantioselective complexation, it is challenging to develop a chiral receptor capable of showing excellent chiral recognition/discrimination based on the π–π stacking interaction.

Recently, we have reported the design and synthesis of chiral diporphyrin receptor **1** (Figure 1).[11] Because this is the first example of positioning two porphyrins in a parallel but chiral manner at a distance suitable for sandwiching aromatic molecules, the function of **1** is worthy of investigation even if a large number of porphyrin dimers have been reported for various purposes.[12] We found that **1**, which has a macrocyclic cavity to include aromatic guest molecules via cooperative double π–π stacking interactions, enabled the naked-eye detection of an aromatic explosive as well as chiral discrim-

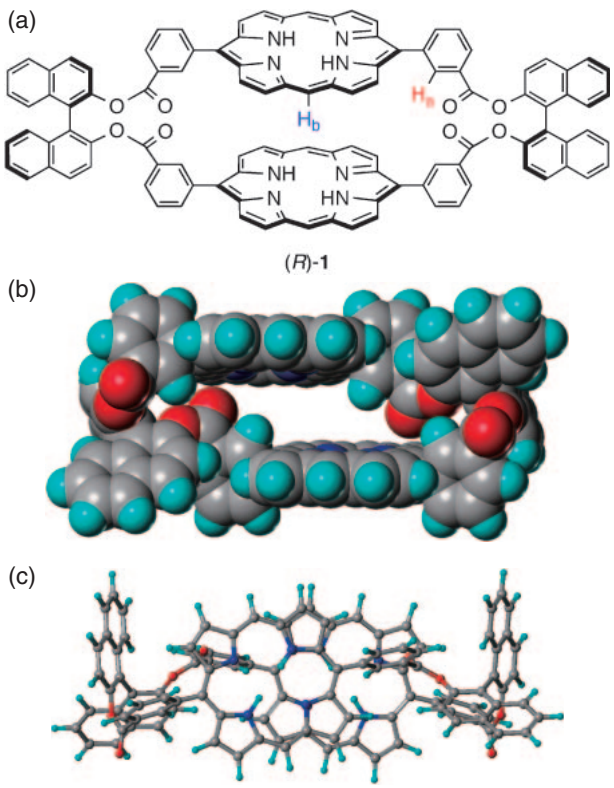

Figure 1. (a) Chemical and (b), (c) optimized structures of (*R*)-**1**. NMR complexation-induced shifts ($\Delta\delta$) for the H_a and H_b atoms are shown in Figure 3. The geometry was optimized by MM3 calculations with CAChe WorkSystem Pro ver. 5.02 (Fujitsu).

Published on the web December 30, 2011; doi:10.1246/bcsj.20110230

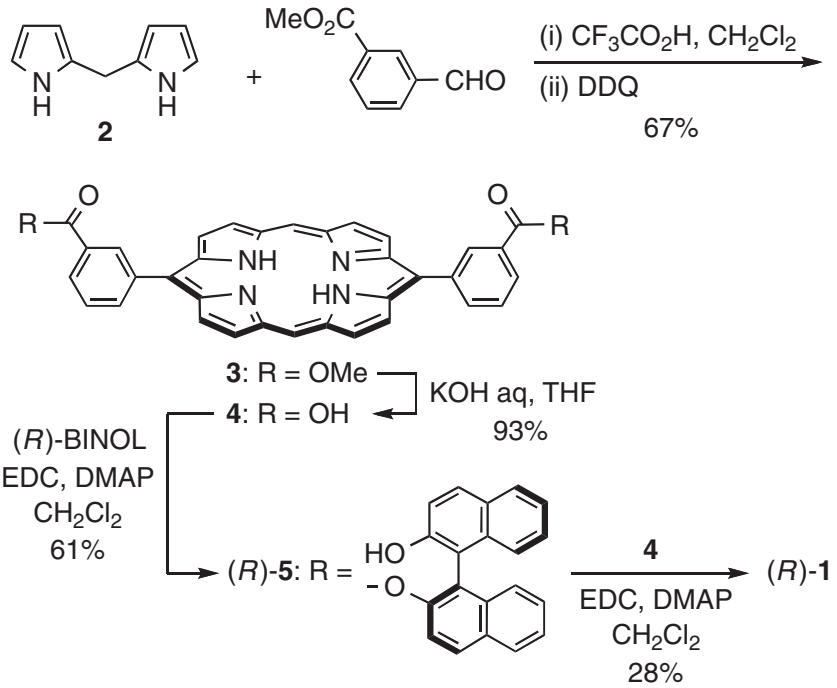

Scheme 1. Synthesis of chiral receptor (*R*)-**1**.

ination by NMR spectroscopy. Here we report the binding and chiral discriminating abilities of **1** in detail.

Results and Discussion

We designed chiral receptor **1** based on the following strategies. First, two porphyrins, which have rigidity, a large π-surface, and a great ring-current effect, were disposed in parallel at a distance of ca. 7 Å suitable for the inclusion of aromatic guests. Second, chiral spacers were used to link the two porphyrins, forming a chiral cavity. BINOL was considered to be a good spacer because of moderate rigidity/flexibility and the ring-current effect. Molecular mechanics (MM) calculations indicated that the two porphyrins in **1** are arranged in an offset face-to-face geometry with an interplanar distance of 5.8–7.2 Å, which is suitable for the intercalation of aromatic molecules (Figure 1). We also expected that the macrocyclic framework would be useful for the restriction of the orientation of the bound guest, which would be favorable for chiral discrimination, and for the suppression of self-aggregation of the receptor. The synthesis of **1** could be achieved easily in five steps from pyrrole (Scheme 1).[11] The stepwise macrocyclization with **4** and **5** to give **1** was found to be much more efficient than the direct macrocyclization with **4** and BINOL to give **1**. In the synthesis of **5**, we observed that the second esterification of the two hydroxy groups in BINOL proceeded much more slowly than the first esterification, which allowed us to obtain **5** selectively. It seemed that the use of the isolated intermediate **5** was important for the subsequent macrocyclization to occur cleanly. It is interesting that such a sophisticated receptor **1** could be constructed easily by using the relatively simple porphyrin **4** and the commercially available BINOL.

We investigated whether **1** could bind aromatics as expected. The aromatic compounds **G1**–**G10** were selected as guests (Figure 2). Complexation of **1** with **G1**–**G7** and **G9**–**G10** in

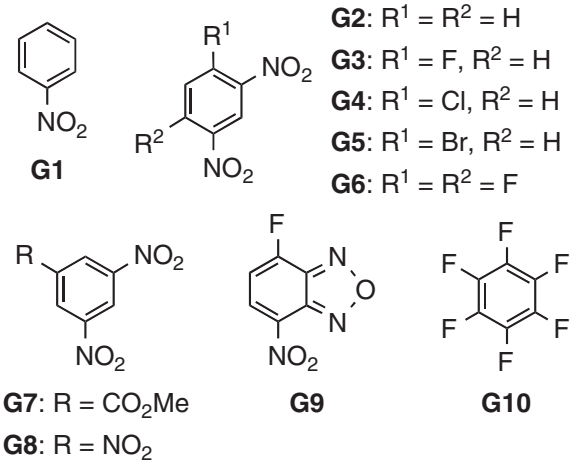

Figure 2. Guest compounds.

$CDCl_3$ was monitored at 25 °C by ^{1}H NMR. Upon addition of any guest, the H_a signal underwent an upfield shift, while the H_b signal experienced a downfield shift, as represented in Figures 3a and 3b (H_a and H_b atoms are designated in Figure 1). The binding constants (K_a) were determined by NMR titration; a nonlinear least-squares method was applied to the H_a signal that was upfield shifted upon addition of the guest (Figure 3b).[13] As for **G8**, the K_a value was determined by UV–vis titration (Figure 4); the absorbance change at 505 nm was used for the curve fitting. The data are listed in Table 1.

The K_a value increases in the following order: **G1** < **G2** < **G3** < **G6** < **G8**. This trend indicates the greater affinity of π-basic **1** for more electron-deficient, π-acidic aromatic guests. The complexation between **1** and **G8** ($K_a = 1850\,M^{-1}$) was stronger by $-2.2\,kcal\,mol^{-1}$ than that between porphyrin

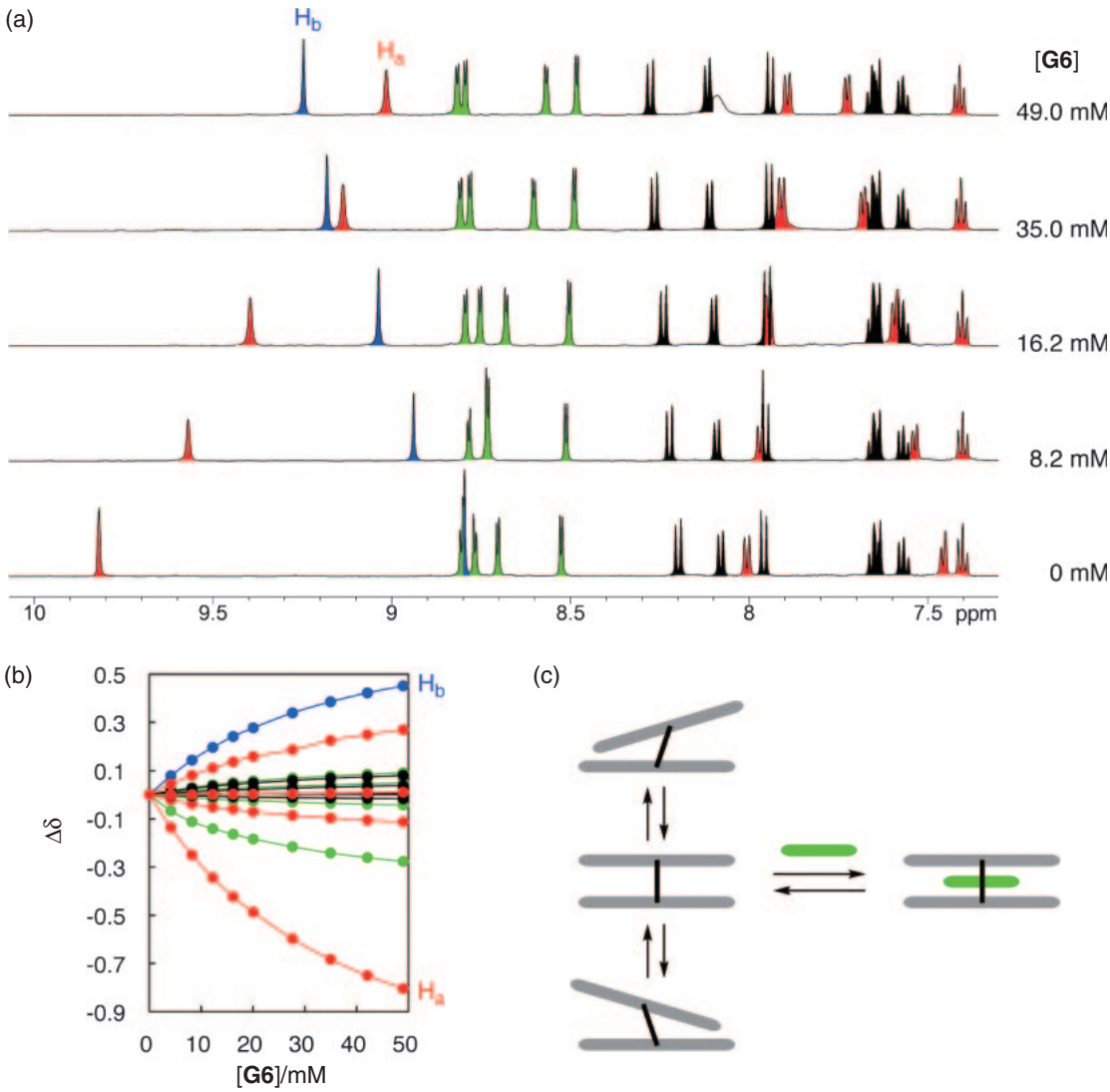

Figure 3. (a) Complexation-induced shifts ($\Delta\delta$) for all the aromatic protons of (*R*)-**1** (10 mM) as a function of [**G6**] in $CDCl_3$ at 25 °C. The H_a and H_b atoms are designated in Figure 1. The signals for the *meso*-phenyl groups, the pyrrolic β protons, and the binaphthyl groups are shown in red, green, and black, respectively. (b) Plots of the $\Delta\delta$ values for the aromatic protons of (*R*)-**1** as a function of [**G6**]. (c) Plausible conformational change of **1** deduced by the NMR titration. The porphyrin rings and the chiral spacers are represented by the gray and black bars, respectively, while the aromatic guest is represented by the green bar.

monomer **3** and **G8** ($K_a = 50\,M^{-1}$), and the former ($\Delta H° = -8.4\,kcal\,mol^{-1}$, $T\Delta S° = -4.0\,kcal\,mol^{-1}$ at 25 °C) was more enthalpy-driven than the latter ($\Delta H° = -5.7\,kcal\,mol^{-1}$, $T\Delta S° = -3.4\,kcal\,mol^{-1}$ at 25 °C). These results strongly suggest that **G8** was intercalated into the cavity of **1** via the cooperative double π–π stacking. The K_a values of **1** for the electron-deficient guests **G7** and **G9** were reasonably high, whereas that for **G10**, which is electron-deficient enough, was much lower than expected. The latter result may be due to the steric hindrance caused by the limited size of the cavity in **1**. Table 1 also indicates that the K_a value decreases in the following order: **G2** > **G4** > **G5**. This is also due to the steric hindrance of the halogen atom (H < Cl < Br). Although we expected the CH/π interactions for cyclohexane, the K_a value was too small to determine, which suggests that **1** has a specific cavity where only aromatic molecules bearing the nitro groups can be nicely included.

As we have reported previously,[11] the H_b signal for **1** (8.83 ppm) appeared at a higher magnetic field than expected, which becomes clear by comparison with the corresponding signal for **5** (10.32 ppm). This suggests that **1** takes a conformation where the edge of one porphyrin ring is close to the other one as shown in Figure 3c. Because a single H_b signal was observed (Figure 3a), **1** experienced a fast conformational change (Figure 3c). On the other hand, the H_a signal appeared at a much lower magnetic field than expected, which may be due to a specific conformation of the adjacent C=O group. Upon inclusion of a guest molecule, the two porphyrin rings become parallel, which makes the chemical shifts of the H_a and H_b atoms in **1** come closer to those of the corresponding atoms in **5**. Although the ring-current effect of the included aromatic guest molecule may also affect the chemical shifts of the H_a and H_b atoms in **1**, the effect of the conformational change of **1** seems to be predominant. Such a

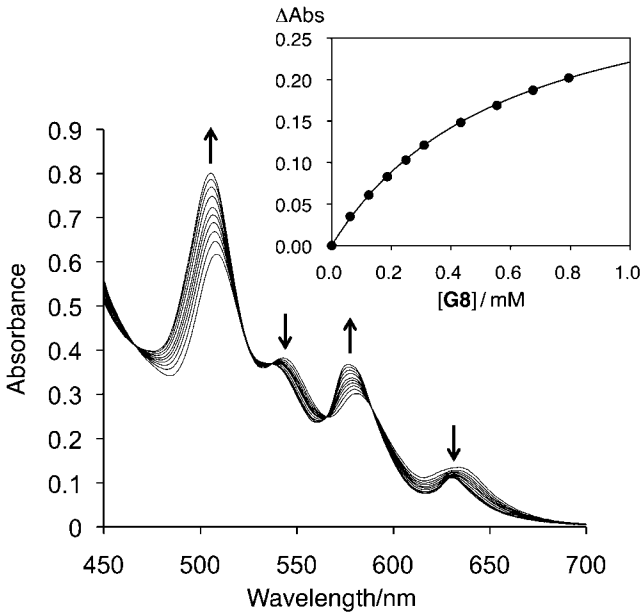

Figure 4. UV–vis spectral change of (*R*)-**1** (50 μM) upon addition of **G8** (0–0.8 mM) in $CHCl_3$. The inset shows the absorbance change at 505 nm with a curve fitting.

Table 1. Binding Constants of (*R*)-**1** for Aromatic Guests

Guest	K_a/M^{-1} a)	$\Delta G°$/kcal mol^{-1} b)
G1	0.1	+1.4
G2	7.7	−1.2
G3	15.2	−1.6
G4	5.8	−1.0
G5	3.6	−0.8
G6	35.8	−2.1
G7	42.9	−2.2
G8	1850c)	−4.5
G9	28.5	−2.0
G10	0.6	+0.3
(*R*)-**G11**	4.2	−0.8
(*S*)-**G11**	1.2	−0.1

a) In chloroform at 25 °C. Determined by NMR titration except for **G8** (UV–vis titration). b) Calculated from $\Delta G° = -RT\ln K_a$. c) The K_a value determined by the NMR titration at a dilute concentration of (*R*)-**1** (50 μM) was 1610.

conformational change can also explain the relatively small binding constants of **1** for the aromatic compounds (Table 1). Most signals for the *meso*-phenyl group exhibited relatively large complexation-induced shifts, whereas the signals for the binaphthyl group showed little or no changes (Figures 3a and 3b). These behaviors suggest that the conformational change of **1** is caused by the tilting movement around (i) the C–C bonds at the *meso*-positions and (ii) the ester bonds.

Unexpectedly, we noticed the formation of precipitates only when **G8**, which is an explosive that is more powerful than 2,4,6-trinitrotoluene (TNT), was added to a solution of **1** in $CDCl_3$ during the NMR titration experiment. Because the development of chemosensors for aromatic explosives has been a challenging subject,[14,15] we investigated the utility of **1** as a chemosensor for **G8**. As shown in Figure 5, a dark-red solution

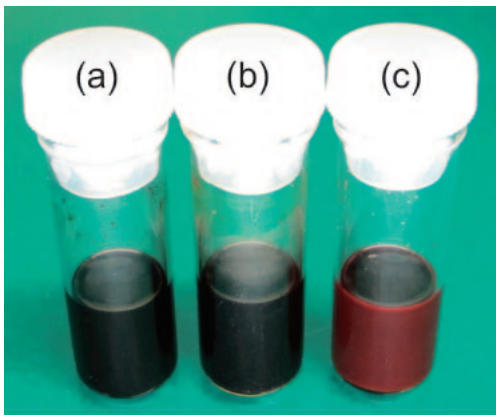

Figure 5. The naked-eye detection of explosive **G8**. (a) A solution of (*R*)-**1** (10 mM) in $CHCl_3$. (b) After addition of **G7** as a control (1 equiv). (c) After addition of **G8** (1 equiv).

of **1** in $CHCl_3$ turned into a suspension upon addition of **G8** (10 mM, 1 equiv), and the light illuminated from the front side was scattered (Figure 5c). This phenomenon was observed only for **G8**; for example, no visual change occurred when **G7** was added to a solution of **1** in $CHCl_3$ (Figure 5b). Thus, **1** acted as a unique naked-eye explosive sensor. We were intrigued with the driving force of the formation of the suspension (Figure 5c). It is unlikely that **G8** included in the cavity of **1** contributed directly to the insolubility of the whole complex. We speculate that the formation of the tight inclusion complex suppressed the flexibility and/or mobility of the porphyrin rings, which triggered a linear intercomplex (supramolecular aggregate) formation that was dependent on the concentration, although the detailed structure of the supramolecular aggregate remains to be investigated. On the other hand, fluorescence spectroscopy was also useful for the selective detection of **G8** (Figure 6). When **G8** was added to a dilute solution of **1** (50 μM), no precipitates appeared, and fluorescence quenching of **1** was observed with excitation at 537 nm, which is an isosbestic point observed in the UV–vis titration. The fluorescence intensity at 635 nm decreased by 37% and 91% in the presence of 0.4 and 5.3 mM of **G8**, respectively (Figure 6b). In contrast, the decrease in fluorescence intensity was only 6% in the presence of 5.3 mM of **G2** (not shown). Figure 6c clearly demonstrates that **1** is a good naked-eye sensor for **G8**.

We evaluated the chiral discrimination ability of **1**. Because **1** showed moderate affinity for dinitrobenzene derivatives (Table 1), we converted alcohols, an amine, and ketones into 3,5-dinitrobenzoyl esters, a 3,5-dinitrobenzoyl amide, and 2,4-dinitrophenylhydrazones, respectively. NMR spectra for the 1:1 mixtures of (*R*)-**1** and **G11**–**G22** (10 mM) were measured in $CDCl_3$. The results are summarized in Table 2. In all cases, host–guest complexation is a fast-exchange equilibrium, where the observed signal is the weighted average of the chemical shift values for unbound and bound enantiomers. As shown in Table 2, chiral discrimination of **G11**–**G22** was successfully achieved by **1**. Host **1**, having no aliphatic hydrocarbon groups that may interfere with the NMR signals for the guests, has a wide detection window (ca. 0–7 ppm), which is advantageous

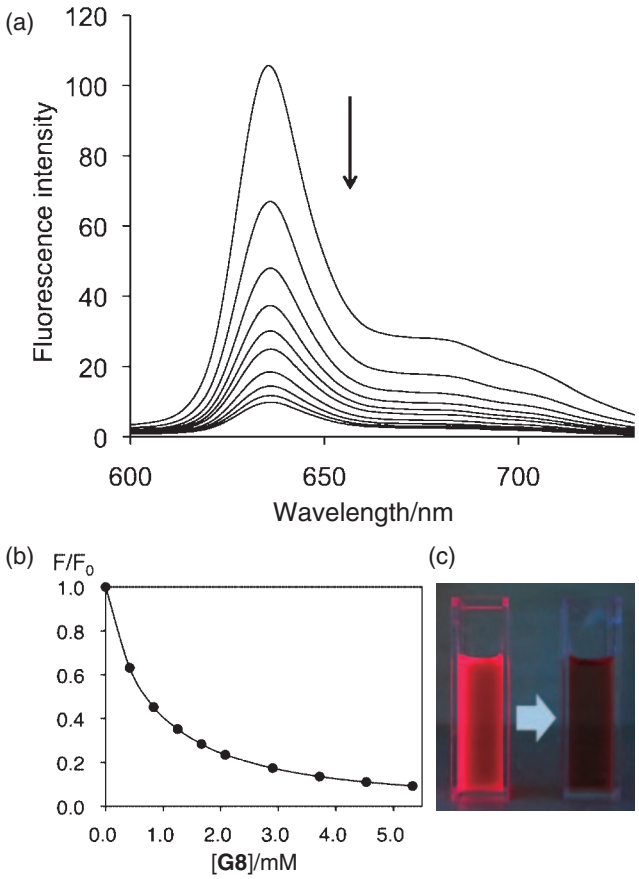

Figure 6. (a) Fluorescence quenching of (*R*)-**1** (50 μM) in $CHCl_3$ upon addition of **G8** (0–5.3 mM). $\lambda_{ex} = 537$ nm. (b) Fluorescence change at 635 nm. (c) Fluorescence before and after addition of **G8** (5.3 mM). $\lambda_{ex} = 365$ nm.

to the analysis of a broad range of chiral compounds. In addition to esters **G11**–**G14** with the methyl group at the stereocenter, esters **G15**–**G19** with two aryl groups at the stereocenter could also be analyzed well, among which **G18** and **G19** were differentiated by ^{19}F NMR. The signal for amide **G20** was also resolved completely. The signals for the methyl group of the R enantiomers of **G11**–**G13** and **G20** appeared at a higher magnetic field. The signals for the two methyl groups of **G21** and for the olefinic proton of **G22** were split. Thus, excellent chiral discrimination has been achieved despite the use of only π–π stacking as a driving force of complexation. We confirmed that a linear correlation exists between the theoretical and observed % ee values (Figure 7). When the effect of the amount of **1** on the signal separation was examined, increasing the amount of **1** increased the degree of the signal separation (Figure 8). These results indicate that **1** can be used as a reagent for the determination of the enantiomeric purity. The following control experiments were also done: when 1-phenylethanol and the corresponding benzoate ester were used as guests instead of **G11**, the signals were not split by **1** at all, probably because of very low affinity. When **5** was used as a chiral host for **G11**, no chiral discrimination was attained, which indicates that the specific cavity in **1** is essential for binding and chiral discrimination of the guest.

After we had obtained the results in Table 2, we determined the K_a values of (*R*)-**1** for (*R*)-**G11** and (*S*)-**G11** to investigate the mechanism of chiral discrimination by NMR spectroscopy. As shown in Table 1, the K_a values were very small ($K_a = 4.2\,M^{-1}$ for (*R*)-**G11** and $K_a = 1.2\,M^{-1}$ for (*S*)-**G11**), which suggests that **G11** is sterically more hindered than the corresponding methyl ester **G7**. The percentages of the host–guest complex ([complex]/[**1**]$_0$) at 10 mM can be calculated to be 3.8% and 1.1% for (*R*)-**G11** and (*S*)-**G11**, respectively. We were therefore surprised to see that chiral discrimination (Table 2 and Figure 8) was possible, based on such weak binding, even if the degree of enantioselectivity was moderate ($K_a(R)/K_a(S) = 3.5$). Upon complexation with (*R*)-**1**, the signal for (*R*)-**G11** shifted to a higher magnetic field than that for (*S*)-**G11** (Table 2 and Figure 8). We suppose that this chiral discrimination by NMR spectroscopy was achieved by the enantioselective binding although the difference in geometry might also be important as described below.

We performed computational calculations to study the inclusion behavior in more detail. Because the π–π stacking interaction involves London dispersion force, it is ideal to perform the ab initio calculations at the highest level. However, because rigorous calculations for such a large molecule are not realistic, we searched for an alternative method using **G7** as a guest. When the semiempirical MO calculations such as the PM3 and PM5 methods were performed, initial complexes converged into unbound structures with the guest molecule evicted. On the other hand, the MM calculations with the MM3 force field turned out to give a stable inclusion complex. An optimized structure is shown in Figures 9a and 9b. The aromatic guest molecule **G7** is closely sandwiched by the two porphyrins, whose interplanar distance is 6.4–7.2 Å. The conformation of **1** is slightly altered upon complexation presumably due to an induced-fit. As shown in Figure 1, the two H_a atoms in **1** are directed inside to create a relatively small cavity. As a result, (i) the nitro group most deeply inserted acts as an anchor, restricting the orientation of **G7** (Figure 9b), and (ii) the alkoxy group in **G7** is located in proximity to the binaphthyl moiety (Figure 9a). These two factors must be important for chiral discrimination (Table 2). To investigate the mechanism of chiral discrimination, we performed the calculations on the complexes between **1** and **G11**. The optimized structures are shown in Figures 9c and 9d. The 3,5-dinitrobenzoyl group in **G11** is intercalated less deeply and more tilted than that in **G7**, which is due to the bulkiness of **G11**, although the interplanar distances in the (*R*)-**1**–(*R*)-**G11** complex (6.5–7.5 Å) and the (*R*)-**1**–(*S*)-**G11** complex (6.3–7.5 Å) are only slightly longer than that in the **1**–**G7** complex (6.4–7.2 Å). Nevertheless, the 3,5-dinitrobenzoyl group in **G11** is fixed in the same direction as that in **G7**. As a result, the stereocenter of **G11** is close to the binaphthyl moiety in **1**. The methyl group in (*R*)-**G11** points straight to the benzoate moiety at the *meso*-position of **1** (Figure 9c), whereas that in (*S*)-**G11** is located on the periphery of the porphyrin ring (Figure 9d). The former is apparently located in a shielding region. Therefore, these geometries are in agreement with the NMR spectrum that the methyl signal of (*R*)-**G11** appeared at a higher magnetic field than that of (*S*)-**G11** upon complexation with (*R*)-**1**.

Table 2. Selected Regions of NMR Spectra of Racemic Guests **G11**–**G22** in the Presence of (*R*)-**1**[a)]

Guest	Spectrum	Guest	Spectrum
G11	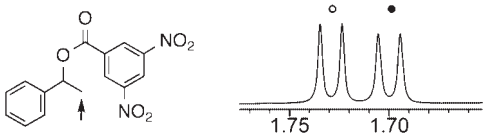	**G17**	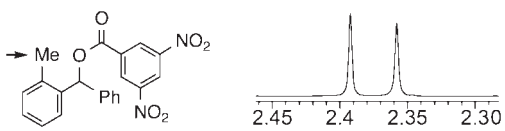
G12	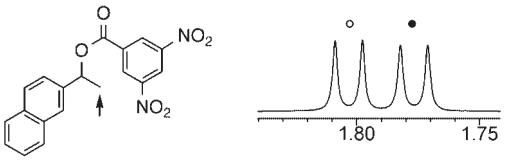	**G18**	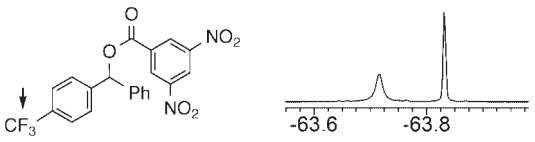
G13	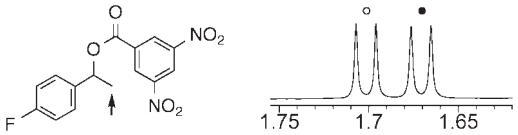	**G19**	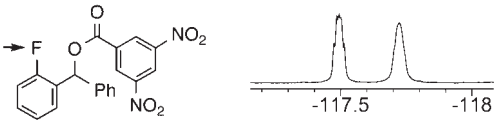
G14	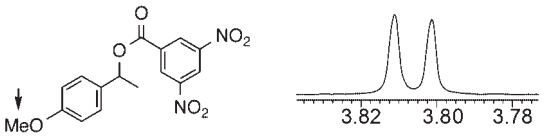	**G20**	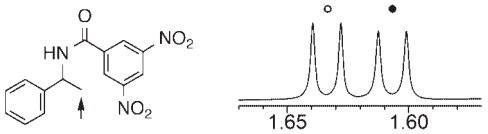
G15	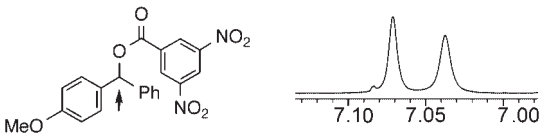	**G21**	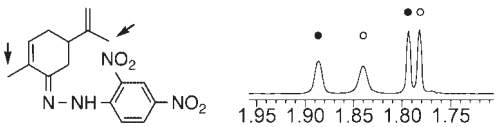
G16	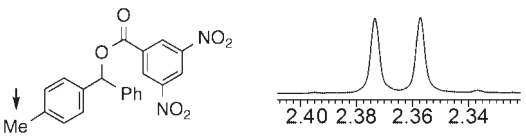	**G22**	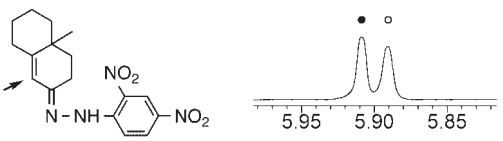

a) 600 MHz ^{1}H NMR of **G11**–**G17** and **G20**–**G22** and 565 MHz ^{19}F NMR of **G18**–**G19** in the presence of (*R*)-**1** (10 mM, 1 equiv) in $CDCl_3$ at 22 °C. The resonances for the protons or fluorines indicated by the arrows are shown in the right column. In the case where the signals for the enantiomers were assigned by adding some amount of one enantiomer to the above solution, (*R*)- and (*S*)-enantiomers are represented by filled and open circles, respectively.

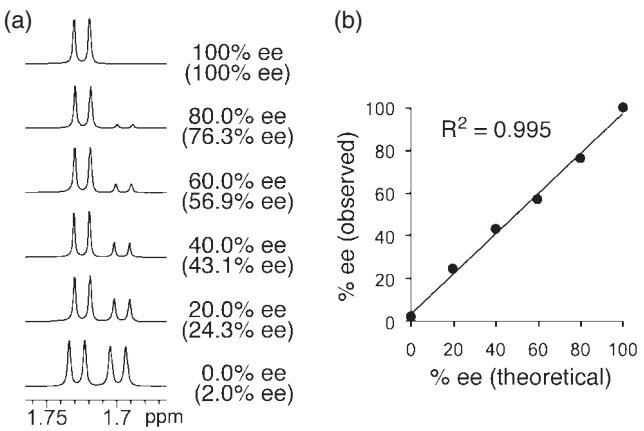

Figure 7. (a) A selected region of 600 MHz ^{1}H NMR of (*S*)-**G11** (1.9 mg, 10 mM) with various enantiomeric purities in the presence of (*R*)-**1** (9.6 mg, 10 mM) in $CDCl_3$ (0.6 mL) at 22 °C. Observed % ee values calculated from the integrals are indicated in the parentheses. (b) Correlation between the theoretical and observed % ee values.

Conclusion

We searched for a chiral receptor exerting an excellent chiral recognition/discrimination power by using the π–π stacking as the driving force of complexation. Such a chiral receptor will widen the scope of application in the field of chiral analysis. Here we have designed and synthesized chiral porphyrin dimer **1** with a macrocyclic cavity suitable for the intercalation of aromatics. It should be noted that **1** has no aliphatic hydrocarbon groups and that such a specific structure could be constructed in only five steps from pyrrole. The binding constants determined indicated that **1** had greater affinity for more electron-deficient aromatic guests. In fact, **1** showed a good ability to discriminate the enantiomers of chiral compounds bearing a dinitrophenyl group by NMR spectroscopy. Unexpectedly, **1** also functioned as a naked-eye sensor for explosive, 1,3,5-trinitrobenzene (**G8**). Therefore, we also expect various applications of **1**.

Experimental

Materials. The receptor **1** and guests **G11**, **G12**, **G20**, and **G21** were prepared as reported previously.[11] The aromatic compounds **G1**–**G10** and all the synthetic reagents and solvents were purchased.

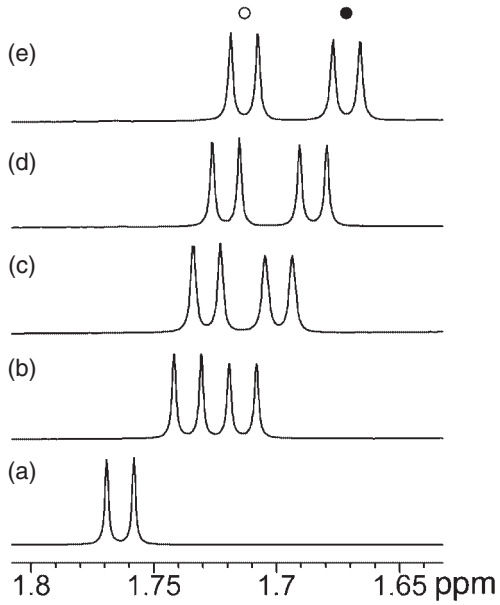

Figure 8. 600 MHz ^{1}H NMR of *rac*-**G11** (1.9 mg, 10 mM) in the presence of (*R*)-**1** (0–15 mM) in $CDCl_3$ (0.6 mL) at 22 °C. (*R*)-**1**: (a) no addition; (b) 0.75 equiv; (c) 1.0 equiv (9.6 mg); (d) 1.25 equiv; (e) 1.5 equiv. Filled and open circles represent (*R*)- and (*S*)-enantiomers, respectively.

Typical Procedure for the Preparation of G13–G19. To a solution of 3,5-dinitrobenzoyl chloride (553 mg, 2.40 mmol) in pyridine (1.6 mL) under N_2 in an ice bath was added the corresponding alcohol (2.10 mmol). The mixture was stirred at room temperature overnight. The reaction was quenched with water, and the product was extracted with EtOAc. The organic layer was dried over $MgSO_4$, and concentrated.

1-(4-Fluorophenyl)ethyl 3,5-Dinitrobenzoate (G13): Purification by silica gel column chromatography (hexane/EtOAc (6:1)) afforded **G13** as colorless crystals (63%): mp 117–119 °C; ^{1}H NMR ($CDCl_3$, 400 MHz): δ 1.75 (d, J = 6.4 Hz, 3H), 6.20 (q, J = 6.4 Hz, 1H), 7.07–7.11 (m, 2H), 7.44–7.48 (m, 2H), 9.15 (d, J = 2.2 Hz, 2H), 9.22 (t, J = 2.2 Hz, 1H); ^{13}C NMR ($CDCl_3$, 100 MHz): δ 21.9, 74.8, 115.7 (d, J = 21.5 Hz), 122.4, 128.3 (d, J = 8.2 Hz), 129.4, 134.0, 135.9 (d, J = 3.0 Hz), 148.6, 161.7, 162.7 (d, J = 246.9 Hz); IR (KBr): 3098, 3051, 2986, 2878, 1732, 1628, 1605, 1543, 1512, 1454, 1346, 1277, 1227, 1165, 1061, 1003, 922, 841, 721 cm^{-1}; Anal. Calcd for $C_{15}H_{11}FN_2O_6$: C, 53.90; H, 3.32; N, 8.38%. Found: C, 53.62; H, 3.35; N, 8.23%; HRMS (EI): calcd for $C_{15}H_{11}FN_2O_6$ 334.0601, found 334.0620 (M^+).

1-(4-Methoxyphenyl)ethyl 3,5-Dinitrobenzoate (G14): Purification by silica gel column chromatography (hexane/EtOAc (3:1)) afforded **G14** as a yellow oil (65%):[16] ^{1}H NMR ($CDCl_3$, 400 MHz): δ 1.75 (d, J = 6.6 Hz, 3H), 3.82 (s, 3H), 6.19 (q, J = 6.6 Hz, 1H), 6.91–6.94 (m, 2H), 7.40–7.43 (m, 2H), 9.14 (d, J = 2.2 Hz, 2H), 9.21 (t, J = 2.2 Hz, 1H); ^{13}C NMR ($CDCl_3$, 100 MHz): δ 21.6, 55.3, 75.3, 114.0, 122.2, 127.9, 129.4, 132.1, 134.3, 148.5, 159.8, 161.8; IR (KBr): 3101, 2970, 2937, 2839, 1728, 1628, 1612, 1549, 1516, 1460, 1344, 1248, 1169, 1057, 1032, 997, 922, 833, 773, 721 cm^{-1}; HRMS (EI): calcd for $C_{16}H_{14}N_2O_7$ 346.0801, found 346.0784 (M^+).

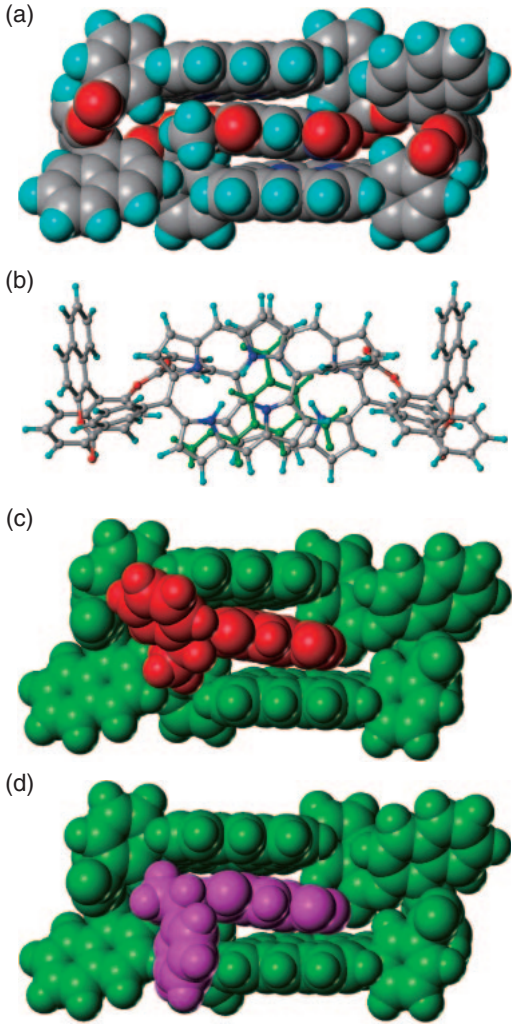

Figure 9. (a) Side view and (b) top view of the (*R*)-**1**–**G7** complex. Side views of (c) the (*R*)-**1**–(*R*)-**G11** complex and (d) the (*R*)-**1**–(*S*)-**G11** complex, where the macrocyclic moiety is shown in green, and (*R*)-**G11** and (*S*)-**G11** are shown in red and magenta, respectively. The geometries were optimized by MM3 calculations with CAChe Work-System Pro ver. 5.02 (Fujitsu).

4-Methoxybenzhydryl 3,5-Dinitrobenzoate (G15): Purification by silica gel column chromatography (hexane/EtOAc (7:1)) afforded **G15** as a slightly yellow viscous oil (69%):[17] ^{1}H NMR ($CDCl_3$, 400 MHz): δ 3.81 (s, 3H), 6.90–6.94 (m, 2H), 7.18 (s, 1H), 7.28–7.44 (m, 7H), 9.21 (d, J = 2.4 Hz, 2H), 9.23 (t, J = 2.4 Hz, 1H); ^{13}C NMR ($CDCl_3$, 100 MHz): δ 55.3, 79.4, 114.1, 122.5, 126.9, 128.4, 128.7, 129.0, 129.5, 130.9, 134.0, 139.0, 148.6, 159.8, 161.7; IR (neat): 3099, 2955, 2854, 1732, 1628, 1611, 1545, 1514, 1460, 1346, 1271, 1250, 1163, 1076, 1032, 920, 829, 721, 700 cm^{-1}; HRMS (EI): calcd for $C_{21}H_{16}N_2O_7$ 408.0958, found 408.0977 (M^+).

4-Methylbenzhydryl 3,5-Dinitrobenzoate (G16): Purification by silica gel column chromatography (hexane/EtOAc (7:1)) afforded **G16** as a yellow foam (86%): ^{1}H NMR ($CDCl_3$, 400 MHz): δ 2.36 (s, 3H), 7.18 (s, 1H), 7.21 (d, J = 8.0 Hz, 2H), 7.33 (d, J = 8.0 Hz, 2H), 7.34–7.45 (m, 5H), 9.21 (d, J = 2.0 Hz, 2H), 9.24 (t, J = 2.0 Hz, 1H); ^{13}C NMR ($CDCl_3$,

100 MHz): δ 21.1, 79.6, 122.5, 127.1, 127.3, 128.4, 128.7, 129.46, 129.48, 133.9, 135.8, 138.5, 138.9, 148.6, 161.7; IR (neat): 3099, 3032, 2916, 1732, 1630, 1545, 1514, 1458, 1346, 1267, 1163, 1076, 920, 821, 739, 721, 700 cm^{-1}; HRMS (EI): calcd for $C_{21}H_{16}N_2O_6$ 392.1008, found 392.1001 (M^+).

2-Methylbenzhydryl 3,5-Dinitrobenzoate (G17): Purification by silica gel column chromatography (hexane/EtOAc (7:1)) afforded **G17** as a slightly yellow viscous oil (27%): ^{1}H NMR ($CDCl_3$, 400 MHz): δ 2.38 (s, 3H), 7.21–7.30 (m, 4H), 7.33–7.38 (m, 5H), 7.39–7.51 (m, 1H), 9.21 (d, $J = 2.2$ Hz, 2H), 9.24 (t, $J = 2.2$ Hz, 1H); ^{13}C NMR ($CDCl_3$, 100 MHz): δ 19.5, 77.02, 122.5, 126.4, 126.7, 127.7, 128.5, 128.6, 128.8, 129.5, 130.9, 133.9, 135.8, 136.8, 138.0, 148.7, 161.7; IR (neat): 3099, 3030, 2943, 2880, 1732, 1630, 1599, 1545, 1495, 1456, 1344, 1261, 1161, 1074, 1030, 920, 872, 847, 812, 791, 698 cm^{-1}; HRMS (EI): calcd for $C_{21}H_{16}N_2O_6$ 392.1008, found 392.1003 (M^+).

4-(Trifluoromethyl)benzhydryl 3,5-Dinitrobenzoate (G18): Purification by silica gel column chromatography (hexane/EtOAc (7:1)) afforded **G18** as a slightly yellow viscous oil (65%): ^{1}H NMR ($CDCl_3$, 400 MHz): δ 7.23 (s, 1H), 7.39–7.44 (m, 5H), 7.57 (d, $J = 8.2$ Hz, 2H), 7.67 (d, $J = 8.2$ Hz, 2H), 9.22 (d, $J = 2.2$ Hz, 2H), 9.26 (t, $J = 2.2$ Hz, 1H); ^{13}C NMR ($CDCl_3$, 100 MHz): δ 78.9, 122.7, 123.8 (q, $J = 270.8$ Hz), 125.8 (q, $J = 3.7$ Hz), 127.3, 127.4, 129.02, 129.04, 129.5, 130.7 (q, $J = 32.0$ Hz), 133.5, 137.9, 142.7, 148.7, 161.6; IR (KBr): 3101, 3036, 2943, 2882, 1740, 1628, 1543, 1497, 1458, 1420, 1342, 1327, 1273, 1165, 1126, 1069, 1018, 968, 918, 833, 806, 772, 721, 698 cm^{-1}; HRMS (EI): calcd for $C_{21}H_{13}F_3N_2O_6$ 446.0726, found 446.0728 (M^+).

2-Fluorobenzhydryl 3,5-Dinitrobenzoate (G19): Purification by silica gel column chromatography (hexane/EtOAc (7:1)) afforded **G19** as colorless crystals (64%): mp 140–141 °C; ^{1}H NMR ($CDCl_3$, 400 MHz): δ 7.09–7.14 (m, 1H), 7.18–7.22 (m, 1H), 7.33–7.48 (m, 8H), 9.21 (d, $J = 2.2$ Hz, 2H), 9.25 (t, $J = 2.2$ Hz, 1H); ^{13}C NMR ($CDCl_3$, 100 MHz): δ 74.0 (d, $J = 2.9$ Hz), 116.0 (d, $J = 21.6$ Hz), 122.6, 124.5 (d, $J = 3.7$ Hz), 126.2 (d, $J = 12.7$ Hz), 127.0, 128.2 (d, $J = 3.0$ Hz), 128.7, 128.8, 129.5, 130.4 (d, $J = 8.9$ Hz), 133.7, 137.6, 148.7, 160.1 (d, $J = 247.6$ Hz), 161.4; IR (KBr): 3105, 3032, 2882, 1728, 1632, 1585, 1543, 1489, 1454, 1346, 1280, 1231, 1165, 1076, 1030, 972, 914, 814, 760, 721, 694 cm^{-1}; Anal. Calcd for $C_{20}H_{13}FN_2O_6$: C, 60.61; H, 3.31; N, 7.07%. Found: C, 60.37; H, 3.22; N, 6.80%; HRMS (EI): calcd for $C_{20}H_{13}FN_2O_6$ 396.0758, found 396.0753 (M^+).

6-Methylbicyclo[4.4.0]dec-1-en-3-one 2,4-Dinitrophenylhydrazone (G22): To a solution of 2,4-dinitrophenylhydrazine (170 mg, 0.86 mmol) in EtOH (30 mL) was added 5 drops of H_2SO_4, and the mixture was heated until 2,4-dinitrophenylhydrazine was dissolved. After cooling, a solution of the corresponding ketone (0.86 mmol) in EtOH (4 mL) and H_2O (2 mL) was added, and the mixture was stirred at room temperature. The reaction was monitored by TLC. Saturated aqueous $NaHCO_3$ was added to neutralize the solution, and the product was extracted with CH_2Cl_2. The organic layer was dried over $MgSO_4$, and concentrated. Purification by silica gel column chromatography (hexane/$CHCl_3$ (1:3)) followed by recrystallization from CH_2Cl_2 afforded (*R*)-**G22** as orange crystals (29%).[18] The enantiomer was also prepared in the same way: mp 174–176 °C; $[\alpha]_D^{22}$ −427 (*c* 0.50, $CHCl_3$); ^{1}H NMR ($CDCl_3$, 600 MHz): δ 1.17 (s, 3H), 1.29–1.40 (m, 2H), 1.64–1.72 (m, 4H), 1.80–1.83 (m, 1H), 1.86–1.90 (m, 1H), 2.29–2.36 (m, 2H), 2.43–2.49 (m, 1H), 2.72–2.76 (m, 1H), 6.01 (s, 1H), 7.98 (d, $J = 9.6$ Hz, 1H), 8.29 (dd, $J = 2.4$, 9.6 Hz, 1H), 9.13 (d, $J = 2.4$ Hz, 1H), 11.25 (s, 1H); IR (KBr): 3312, 3117, 2924, 2853, 1622, 1591, 1506, 1418, 1337, 1306, 1254, 1221, 1126, 912, 831, 743 cm^{-1}; HRMS (EI): calcd for $C_{17}H_{20}N_4O_4$ 344.1485, found 344.1487 (M^+).

Determination of Binding Constants. In the NMR titration, to a solution of **1** (10 mM) in $CDCl_3$ (0.6 mL) was added a small amount of $CDCl_3$ containing guest, and ^{1}H NMR spectra were then measured at 25 °C. The change in the H_a signal of **1** was monitored at several different concentrations of guest. On the other hand, in the NMR titration, to a solution of **1** (50 μM) in $CHCl_3$ (3.0 mL) was added a small amount of $CHCl_3$ containing **G8**, and UV–vis spectra were then measured at a constant temperature. The absorbance change at 505 nm was monitored at several different concentrations of **G8**. Several isosbestic points were observed, indicating 1:1 complexation. The binding constant was calculated by the nonlinear least-squares curve-fitting method. The thermodynamic parameters were obtained from the van't Hoff plots.

MM Calculations. MM calculations on (*R*)-**1**, the (*R*)-**1**–**G7** complex, the (*R*)-**1**–(*R*)-**G11** complex, and the (*R*)-**1**–(*S*)-**G11** complex were done with CAChe WorkSystem Pro ver. 5.02 (Fujitsu), where the structures were optimized by the MM3 method.

This work was supported by a Grant for Research for Promoting Technological Seeds from Japan Science and Technology Agency (JST) and by Okayama Foundation for Science and Technology. We thank Takasago International Corporation for providing us with (*S*)-1-(4-fluorophenyl)ethanol. We are grateful to the SC-NMR Laboratory of Okayama University for the measurement of NMR spectra.

References

Dedicated to Emeritus Professor H. Ogoshi (Kyoto University) on the occasion of his 77th birthday.

1 Recent reports on chiral recognition (enantioselective binding): a) G. Fukuhara, S. Madenci, J. Polkowska, F. Bastkowski, F.-G. Klärner, Y. Origane, M. Kaneda, T. Mori, T. Wada, Y. Inoue, *Chem.—Eur. J.* **2007**, *13*, 2473. b) F. Gasparrini, M. Pierini, C. Villani, A. Filippi, M. Speranza, *J. Am. Chem. Soc.* **2008**, *130*, 522. c) S. Bartoli, T. Mahmood, A. Malik, S. Dixon, J. D. Kilburn, *Org. Biomol. Chem.* **2008**, *6*, 2340. d) T. Haino, H. Fukuoka, H. Iwamoto, Y. Fukazawa, *Supramol. Chem.* **2008**, *20*, 51. e) S. Shirakawa, A. Moriyama, S. Shimizu, *Eur. J. Org. Chem.* **2008**, 5957. f) R. Carrillo, M. López-Rodríguez, V. S. Martín, T. Martín, *Angew. Chem., Int. Ed.* **2009**, *48*, 7803. g) M. E. Amato, F. P. Ballistreri, S. Gentile, A. Pappalardo, G. A. Tomaselli, R. M. Toscano, *J. Org. Chem.* **2010**, *75*, 1437.

2 T. J. Wenzel, *Discrimination of Chiral Compounds Using NMR Spectroscopy*, Wiley, New Jersey, **2007**.

3 Recent reports on chiral discrimination in NMR: a) F. Ma, X. Shen, X. Ming, J. Wang, J. Ou-Yang, C. Zhang, *Tetrahedron: Asymmetry* **2008**, *19*, 1576. b) K. Tanaka, N. Fukuda, *Tetrahedron: Asymmetry* **2009**, *20*, 111. c) S. Sambasivan, D. Kim, K. H. Ahn,

Chem. Commun. **2010**, *46*, 541. d) L. S. Moon, M. Pal, Y. Kasetti, P. V. Bharatam, R. S. Jolly, *J. Org. Chem.* **2010**, *75*, 5487. e) D. P. Iwaniuk, C. Wolf, *J. Org. Chem.* **2010**, *75*, 6724. f) E. Busto, A. González-Álvarez, V. Gotor-Fernández, I. Alfonso, V. Gotor, *Tetrahedron* **2010**, *66*, 6070. g) M. Durmaz, M. Yilmaz, A. Sirit, *Org. Biomol. Chem.* **2011**, *9*, 571. h) K. Tanaka, Y. Nakai, H. Takahashi, *Tetrahedron: Asymmetry* **2011**, *22*, 178. i) N. H. Pham, T. J. Wenzel, *J. Org. Chem.* **2011**, *76*, 986.

4 a) T. Ema, D. Tanida, T. Sakai, *Org. Lett.* **2006**, *8*, 3773. b) T. Ema, D. Tanida, T. Sakai, *J. Am. Chem. Soc.* **2007**, *129*, 10591. c) T. Ema, D. Tanida, K. Hamada, T. Sakai, *J. Org. Chem.* **2008**, *73*, 9129. d) T. Ema, D. Tanida, K. Sugita, T. Sakai, K. Miyazawa, A. Ohnishi, *Org. Lett.* **2008**, *10*, 2365. e) T. Ema, K. Hamada, K. Sugita, Y. Nagata, T. Sakai, A. Ohnishi, *J. Org. Chem.* **2010**, *75*, 4492.

5 Reviews and accounts: a) J. H. Williams, *Acc. Chem. Res.* **1993**, *26*, 593. b) C. A. Hunter, K. R. Lawson, J. Perkins, C. J. Urch, *J. Chem. Soc., Perkin Trans. 2* **2001**, 651. c) E. A. Meyer, R. K. Castellano, F. Diederich, *Angew. Chem., Int. Ed.* **2003**, *42*, 1210. d) M. Harmata, *Acc. Chem. Res.* **2004**, *37*, 862.

6 Theoretical studies: a) C. A. Hunter, J. K. M. Sanders, *J. Am. Chem. Soc.* **1990**, *112*, 5525. b) A. P. West, Jr., S. Mecozzi, D. A. Dougherty, *J. Phys. Org. Chem.* **1997**, *10*, 347. c) M. Kamieth, F.-G. Klärner, F. Diederich, *Angew. Chem., Int. Ed.* **1998**, *37*, 3303.

7 a) J. Landauer, H. McConnell, *J. Am. Chem. Soc.* **1952**, *74*, 1221. b) D. M. G. Lawrey, H. McConnell, *J. Am. Chem. Soc.* **1952**, *74*, 6175. c) S. C. Zimmerman, C. M. VanZyl, *J. Am. Chem. Soc.* **1987**, *109*, 7894. d) S. C. Zimmerman, C. M. VanZyl, G. S. Hamilton, *J. Am. Chem. Soc.* **1989**, *111*, 1373. e) T. Korenaga, Y. Kawauchi, T. Kosaki, T. Ema, T. Sakai, *Bull. Chem. Soc. Jpn.* **2005**, *78*, 2175. f) T. Haino, T. Fujii, Y. Fukazawa, *J. Org. Chem.* **2006**, *71*, 2572. g) S. L. Cockroft, J. Perkins, C. Zonta, H. Adams, S. E. Spey, C. M. R. Low, J. G. Vinter, K. R. Lawson, C. J. Urch, C. A. Hunter, *Org. Biomol. Chem.* **2007**, *5*, 1062. h) B. Branchi, V. Balzani, P. Ceroni, M. C. Kuchenbrandt, F.-G. Klärner, D. Bläser, R. Boese, *J. Org. Chem.* **2008**, *73*, 5839. i) B. Legouin, P. Uriac, S. Tomasi, L. Toupet, A. Bondon, P. van de Weghe, *Org. Lett.* **2009**, *11*, 745.

8 a) B. Askew, P. Ballester, C. Buhr, K. S. Jeong, S. Jones, K. Parris, K. Williams, J. Rebek, Jr., *J. Am. Chem. Soc.* **1989**, *111*, 1082. b) B. J. Whitlock, H. W. Whitlock, *J. Am. Chem. Soc.* **1994**, *116*, 2301. c) T. Hayashi, T. Miyahara, N. Koide, Y. Kato, H. Masuda, H. Ogoshi, *J. Am. Chem. Soc.* **1997**, *119*, 7281. d) A. I. Oliva, L. Simón, F. M. Muñiz, F. Sanz, C. Ruiz-Valero, J. R. Morán, *J. Org. Chem.* **2004**, *69*, 6883.

9 a) Y. Shoji, K. Tashiro, T. Aida, *J. Am. Chem. Soc.* **2006**, *128*, 10690. b) Y. Shoji, K. Tashiro, T. Aida, *J. Am. Chem. Soc.* **2010**, *132*, 5928.

10 a) X. Peng, N. Komatsu, S. Bhattacharya, T. Shimawaki, S. Aonuma, T. Kimura, A. Osuka, *Nat. Nanotechnol.* **2007**, *2*, 361. b) X. Peng, N. Komatsu, T. Kimura, A. Osuka, *J. Am. Chem. Soc.* **2007**, *129*, 15947. c) X. Peng, N. Komatsu, T. Kimura, A. Osuka, *ACS Nano* **2008**, *2*, 2045.

11 T. Ema, N. Ura, K. Eguchi, Y. Ise, T. Sakai, *Chem. Commun.* **2011**, *47*, 6090.

12 a) T. Kurtán, N. Nesnas, Y.-Q. Li, X. Huang, K. Nakanishi, N. Berova, *J. Am. Chem. Soc.* **2001**, *123*, 5962. b) T. Kurtán, N. Nesnas, F. E. Koehn, Y.-Q. Li, K. Nakanishi, N. Berova, *J. Am. Chem. Soc.* **2001**, *123*, 5974. c) Y. Kubo, Y. Ishii, T. Yoshizawa, S. Tokita, *Chem. Commun.* **2004**, 1394. d) T. Ema, N. Ouchi, T. Doi, T. Korenaga, T. Sakai, *Org. Lett.* **2005**, *7*, 3985. e) A. Ouchi, K. Tashiro, K. Yamaguchi, T. Tsuchiya, T. Akasaka, T. Aida, *Angew. Chem., Int. Ed.* **2006**, *45*, 3542. f) J. Aimi, K. Oya, A. Tsuda, T. Aida, *Angew. Chem., Int. Ed.* **2007**, *46*, 2031. g) H. Nobukuni, Y. Shimazaki, F. Tani, Y. Naruta, *Angew. Chem., Int. Ed.* **2007**, *46*, 8975. h) H. Uno, K. Nakamoto, K. Kuroki, A. Fujimoto, N. Ono, *Chem.—Eur. J.* **2007**, *13*, 5773. i) Y. Ishii, T. Yoshizawa, Y. Kubo, *Org. Biomol. Chem.* **2007**, *5*, 1210. j) L. Jiao, E. Hao, F. R. Fronczek, K. M. Smith, M. G. H. Vicente, *Tetrahedron* **2007**, *63*, 4011. k) Y. Matano, K. Matsumoto, Y. Nakao, H. Uno, S. Sakaki, H. Imahori, *J. Am. Chem. Soc.* **2008**, *130*, 4588. l) V. Borovkov, T. Yamamoto, H. Higuchi, Y. Inoue, *Org. Lett.* **2008**, *10*, 1283. m) A. Takai, C. P. Gros, J.-M. Barbe, R. Guilard, S. Fukuzumi, *Chem.—Eur. J.* **2009**, *15*, 3110. n) C.-H. Lee, H. Yoon, W.-D. Jang, *Chem.—Eur. J.* **2009**, *15*, 9972. o) J. Song, N. Aratani, J. H. Heo, D. Kim, H. Shinokubo, A. Osuka, *J. Am. Chem. Soc.* **2010**, *132*, 11868. p) C.-L. Mai, W.-K. Huang, H.-P. Lu, C.-W. Lee, C.-L. Chiu, Y.-R. Liang, E. W.-G. Diau, C.-Y. Yeh, *Chem. Commun.* **2010**, *46*, 809. q) H. Nobukuni, Y. Shimazaki, H. Uno, Y. Naruta, K. Ohkubo, T. Kojima, S. Fukuzumi, S. Seki, H. Sakai, T. Hasobe, F. Tani, *Chem.—Eur. J.* **2010**, *16*, 11611.

13 K. A. Connors, *Binding Constants*, Wiley, New York, **1987**.

14 a) D. Zhao, T. M. Swager, *Macromolecules* **2005**, *38*, 9377. b) Y. H. Lee, H. Liu, J. Y. Lee, S. H. Kim, S. K. Kim, J. L. Sessler, Y. Kim, J. S. Kim, *Chem.—Eur. J.* **2010**, *16*, 5895. c) Y. Peng, A.-J. Zhang, M. Dong, Y.-W. Wang, *Chem. Commun.* **2011**, *47*, 4505.

15 For the toxicity of nitroaromatic compounds, see the Web site of the Agency for Toxic Substances and Disease Registry (ATSDR) of the Department of Health and Human Services (Atlanta, Georgia, USA) (http://www.atsdr.cdc.gov/).

16 M. R. Edwards, P. G. Jones, A. J. Kirby, *J. Am. Chem. Soc.* **1986**, *108*, 7067.

17 B. Denegri, O. Kronja, *J. Phys. Org. Chem.* **2009**, *22*, 495.

18 G. Stork, P. Rosen, N. Goldman, R. V. Coombs, J. Tsuji, *J. Am. Chem. Soc.* **1965**, *87*, 275.